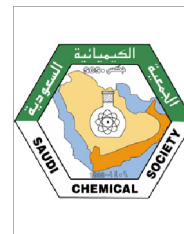




King Saud University
Arabian Journal of Chemistry

www.ksu.edu.sa
www.sciencedirect.com



ORIGINAL ARTICLE

Green synthesis of silver nanoparticles using the seaweed *Gracilaria birdiae* and their antibacterial activity

Anderson Passos de Aragão^a, Taiane Maria de Oliveira^a, Patrick Veras Quelemes^a, Márcia Luana Gomes Perfeito^a, Maria Carvalho Araújo^a, Janaína de Araújo Sousa Santiago^a, Vinicius S. Cardoso^a, Pedro Quaresma^b, José Roberto de Souza de Almeida Leite^a, Durcilene Alves da Silva^{a,*}

^a Núcleo de Pesquisa em Biodiversidade e Biotecnologia, BIOTEC, Campus Ministro Reis Veloso, Universidade Federal do Piauí, UFPI, 64202020 Parnaíba, PI, Brazil

^b REQUIMTE-UCIBIO, Departamento de Química e Bioquímica, Faculdade de Ciências, Universidade do Porto, 4169-007 Porto, Portugal

Received 15 January 2016; accepted 22 April 2016

KEYWORDS

Silver nanoparticles;
Green synthesis;
Algae;
Gracilaria birdiae

Abstract This work presents a simple method for the green synthesis of silver nanoparticles (AgNPs) using as reducing and stabilizing agent a polysaccharide extracted from red algae *Gracilaria birdiae* present in the coast of Piauí. The AgNPs were prepared using three polysaccharide concentrations (0.02, 0.03 and 0.05% v/v) and two pHs (10 and 11) at stirring for 30 min at 90 °C. The formation of silver nanoparticles was monitored by measurements of UV–vis and FTIR and characterized by size and zeta potential measurements using DLS and morphologically by TEM. The UV–vis absorption spectrum showed the surface plasmon peak at 410 nm, which is characteristic peak of silver nanoparticles. The functional biomolecules present in the polysaccharide and the interaction between the nanoparticles were identified by the Fourier transform infrared spectroscopy (FTIR) analysis. The stability of the synthesized silver nanoparticles was analyzed during four months and no significant agglomeration was observed. The hydrodynamic diameter of the AgNPs varied between 20.2 nm and 94.9 nm. The AgNPs were tested for antimicrobial activity using *Escherichia coli* (Gram-negative) and *Staphylococcus aureus* (Gram-positive) and all

* Corresponding author at: Center for Biodiversity Research and Biotechnology (BIOTEC), Federal University of Piauí, Campus Minister Reis Velloso, Parnaíba, Piauí Avenida São Sebastião CEP 64202020, Brazil. Tel.: +55 86 33235433.

E-mail addresses: andersonparagao@gmail.com (A.P. de Aragão), taianeoliveiraphb@gmail.com (T.M. de Oliveira), pquelemes@gmail.com (M.L.G. Perfeito), jrsaleite@gmail.com (J.R. de Souza de Almeida Leite), durcileneas@yahoo.com.br (D.A. da Silva).

Peer review under responsibility of King Saud University.



Production and hosting by Elsevier

<http://dx.doi.org/10.1016/j.arabjc.2016.04.014>

1878-5352 © 2016 The Authors. Production and hosting by Elsevier B.V. on behalf of King Saud University.

This is an open access article under the CC BY-NC-ND license (<http://creativecommons.org/licenses/by-nc-nd/4.0/>).

Please cite this article in press as: de Aragão, A.P. et al., Green synthesis of silver nanoparticles using the seaweed *Gracilaria birdiae* and their antibacterial activity. Arabian Journal of Chemistry (2016), <http://dx.doi.org/10.1016/j.arabjc.2016.04.014>

samples showed antimicrobial activity against *E. coli*. Using an environment-friendly, the AgNPs were synthesized in a simple, rapid and one-step process using natural sources as red algae with favorable characteristics such as spherical shape, small size and zeta potential negative. The results suggest that the polysaccharide mediated synthesized silver nanoparticles could be used as a model for future projects of nano-medicines or drug delivery systems.

© 2016 The Authors. Production and hosting by Elsevier B.V. on behalf of King Saud University. This is an open access article under the CC BY-NC-ND license (<http://creativecommons.org/licenses/by-nc-nd/4.0/>).

1. Introduction

The increased emergence of drug-resistant microbes is a major challenge for the scientific community in the continuous successful development of effective therapeutics. Silver nanoparticles (AgNPs) are known for their antimicrobial properties, being effective against pathogens, which explain their potential for several biotechnological applications, in addition to their electrical, thermal, magnetic, and catalytic characteristics (Chen et al., 2008; Konwarh et al., 2011; Mohanty et al., 2012; MubarakAli et al., 2011; Thakkar et al., 2010; Vigneshwaran et al., 2006).

However, AgNPs show high reactivity, requiring adequate stabilization during and after the process of synthesis to prevent oxidation and aggregation of particles over time. Since the development of the concept of green nanoparticle preparation, there has been growing demand for environment-friendly processes of metal–nanoparticle synthesis that does not employ toxic chemicals (Chen et al., 2008; MubarakAli et al., 2011; Padalia et al., 2015; Thakkar et al., 2010; Thovhogi et al., 2015).

Although several conventional methods of producing pure and well-defined nanoparticles exist, most of these methods are expensive and employ physical processes or chemical reduction with strong reducing agents. In addition, many stabilizers used in these processes, particularly surfactants, may themselves present significant cellular toxicity, which can severely limit the use (Thakkar et al., 2010).

Nanoparticles based noble metals have been produced by green synthesis, using compounds such as ZnO, CdO and Sm₂O₃, among others, without the use of toxic reagents and with the smallest sizes (Diallo et al., 2015; Thema et al., 2015a,b; Thovhogi et al., 2015; Sone et al., 2015). Among the substances used in various methods of synthesis, such as extract and gum, the polysaccharides have been shown to be excellent candidates for stabilizing and controlling the size of nanoparticles (NPs). The stabilization provided by polysaccharides relies on the presence of multiple binding sites along the polysaccharide chain to facilitate attachment to the metal's surface, thereby effectively “trapping” the metal nanoparticle and conferring significant protection against aggregation and chemical modification. Stable silver nanoparticles have been synthesized by the use of polysaccharides, such as starch (Konwarh et al., 2011; Mohanty et al., 2012; Vigneshwaran et al., 2006), chitosan (Tran et al., 2010), natural gums (Gils et al., 2010; Kora et al., 2010; Quelemes et al., 2013), marine polysaccharides (Venkatpurwar and Pokharkar, 2011), and hyaluronan (Xia et al., 2011). In all cases, the polymer plays a dual role as a stabilizer and a reducing agent. This kind of approach allows the use of natural, inexpensive, and biocompatible materials as reducing agents in the synthesis of AgNPs; these agents are capable of providing sufficient stability in therapeutic applications even in the presence of electrolytes and under conditions of pH variation (Wijesekara et al., 2011).

Red marine seaweeds are abundant along the Northeastern Brazilian coast and have high biological potential for providing compounds that have utility in industry, and an example is the *Gracilaria* genus that is common and represents an economic source for the region (Carneiro et al., 2014; Coura et al., 2012). Polysaccharides from the *Gracilaria* genus are composed mainly of the alternating 3-linked-β-D-galactopyranose unit and the 4-linked-3,6-anhydro-α-L-galactopyranose unit (Maciel et al., 2008), where the L moiety may be substituted

by methyl or sulfate groups. The polysaccharide isolated from marine algae has interesting functional properties, such as antioxidant (Souza et al., 2012), anticoagulant, and antiviral activities (Chattopadhyay et al., 2008).

In the present study, silver nanoparticles were prepared using a naturally occurring polysaccharide isolated from red marine algae (*Gracilaria birdiae*), which acted as both the reducing and stabilizing agents. This approach not only utilizes an abundant regional resource, but also falls within the scope of green synthesis for AgNPs that could allow scalability of the process to industrially relevant applications. In addition, we evaluated the antimicrobial activity of the synthesized NPs against representative strains of *Staphylococcus aureus* and *Escherichia coli*.

2. Materials and methods

2.1. Algae polysaccharide extraction

The polysaccharide was isolated from marine red algae (*G. birdiae*) using a reported method (Maciel et al., 2008). The algae were washed to remove impurities, and taken out to dry in the sun. For the extraction of the polysaccharide 5 g of dry seaweed was added to 200 ml of water under stirring for a period of 5 h. The solution was filtered and the pH adjusted to 7.0 with NaOH solution. The polysaccharide was recovered by ethanol precipitation (1:3 v/v), filtered and then washed with ethanol and acetone to remove possible impurities. Finally it was dried under a hot air flow, and the mass obtained was used to calculate the yield. The extracted polysaccharides were characterized by infrared spectroscopy in KBr pellets using a Shimadzu 8300 FT-IR spectrometer. The sulfate content in agar, extracted from the algae, was obtained by inductively coupled plasma optical emission spectrometry (ICP-OES).

2.2. Synthesis of silver nanoparticles

Nanoparticles (AgNPs) were prepared according to method used by Venkatpurwar and Pokharkar (2011) with adaptations. 10 ml of the polysaccharide solution (where the pH of the solutions was adjusted to 10 or 11) was added to 10 ml of an aqueous solution of silver nitrate (AgNO₃) at a concentration of 1 mM under stirring. The reaction was kept under continuous stirring for 30 min and the temperature was brought to 90 °C. Then, the solution was centrifuged at 3600 rpm for 15 min and collected the supernatant. The progress of the reaction was monitored by UV–VIS spectroscopy measurements using a SHIMADZU UV-1800.

2.3. AgNP characterization

The formation of nanostructures was monitored by UV–vis absorption using a Shimadzu (UV 1800) spectrophotometer.

Particle size, zeta potential (ζ) and polydispersity index (PDI) measurements were carried out in a Malvern Zetasizer Nanodynamic light scattering (DLS), Model ZS 3600. The hydrodynamic diameter was measured by dynamic light scattering with a laser with a wavelength of 633 nm and a fixed scattering angle of 173°. The percentage of silver in solution was characterized by the atomic absorption spectroscopy (Varian-Model AA240FS), with wavelength of 328.1 nm and multielement lamp. The reading was held in atomic absorption flame with Oxygen and Acetylene gases.

The stability of AgNPs over time was monitored through UV-vis measurements using the UV-1800 Shimadzu device every 15 days for 4 months. All measurements were performed in triplicate at a constant temperature of $25 \pm 1^\circ\text{C}$. To verify the shape and confirm the diameter of the nanoparticles non-diluted samples of AgNPs (0.03%) for both pHs were placed on two grids (20 μL), for transmission electron microscopy (TEM) previously coated with Form var. After drying for 2 h at room temperature ($25 \pm 2^\circ\text{C}$) the grids were analyzed in a Jeol JEM-1010 electron microscope and photomicrographed by an UltraScan® with Digital Micrograph 3.6.5 software (Gatan/USA). Also characterization was carried out in AgNPs by infrared spectroscopy (FTIR) in KBr pellet of lyophilized nanoparticles using a Shimadzu FT-IR model 8300, in the band 400–4000 cm^{-1} .

2.4. Evaluation of antibacterial activity of AgNPs

To study the antimicrobial activity of AgNPs, two bacterial strains were selected for minimum inhibitory concentration (MIC) determination: *S. aureus* ATCC 29213 (Gram-positive) and *E. coli* ATCC 25922 (Gram-negative) following the methods of Quelemes et al. (2013) and Cardoso et al. (2014). MIC was determined using 96-well microdilution plate with Mueller–Hinton broth where the strains (concentration of 5×10^5 CFU/mL) were exposed to twofold dilution series of AgNPs with silver concentrations ranging from 5.15 μM to 137.5 μM (concentrations determined by atomic absorption spectroscopy). The same procedure to determine the MIC of AgNO_3 with concentrations ranging from 15.62 to 250 μM , and polysaccharide solution with concentrations from 7.8 to 125 $\mu\text{g/mL}$ was used. The plates were incubated for 24 h at 37°C in aerobic conditions. MIC was defined as the lowest concentration of agent that restricted the visual bacterial growth in the culture media.

3. Results and discussion

In the present study, the algal polysaccharide used in the green synthesis of AgNPs played a triple role. The first role was that of forming complexes with the silver ions and thereby controlling the process of reduction. The second role consisted of reducing groups of the polysaccharide while a third role is to stabilize and protect the particles from aggregation. The use of polysaccharides from marine algae has been reported in the literature, when El-Rafie et al. (2013) used a green protocol for the synthesis of silver nanoparticles with polysaccharides extracted from a local variety of algae. In the present study, the seaweed *G. birdiae* was used because it is very commonly found in Northeast Brazil and is therefore an ideal candidate for the process under investigation. A simple procedure to

extract the polysaccharide from the algae was used, which resulted in a yield of 43% and the sulfate content of 2.73% was obtained by inductively coupled plasma optical emission spectrometry (ICP-OES).

The optical properties of the AgNPs allowed us to follow the synthesis by ultraviolet–visible (UV–Vis) spectroscopy. The UV–vis absorption spectra of AgNPs stabilized by the polysaccharide after 2 h of synthesis under various conditions are presented in Fig. 1. The typical band with λ_{max} at 420–400 nm corresponded to the characteristic surface plasmon resonance (SPR) of AgNPs. According to previous reports, the position of SPR absorption of AgNPs depends on their size and shape, as well as the surrounding medium (Zhao et al., 2008) and this particular λ_{max} range is indicative of a spherical shape (Nair and Laurencin, 2007). This finding was further confirmed by transmission electron microscopy (TEM) analysis (Fig. 2).

To determine the influence of polysaccharide concentration and pH on the size and spectra characteristics of the AgNPs, three concentrations (0.02%, 0.03%, and 0.05%) were tested at two different pHs (10 and 11). As the polysaccharide concentration varied from 0.02% to 0.03% the λ_{max} exhibited a blue shift from 420 to 400 nm (Fig. 1). The changes in UV–Vis absorption bands indicated that the size and dispersion of silver nanoparticles were affected by the concentration of polysaccharide and the pH; however, no obvious linear relationship could be inferred from these data. Some authors (Abdel-Mohsen et al., 2014; Kim et al., 2015) demonstrate that varying the polysaccharide concentration and pH can influence the size and aggregation state of the AgNPs and thereby alter the UV–Vis spectra.

The stability of the synthesized silver nanoparticles was analyzed by storing the samples at a temperature of $\sim 25^\circ\text{C}$ for four months. The absorbance at 410 nm was monitored at intervals of 15 days to check for agglomeration. No significant change (at 1.0% level) in absorbance was observed during storage, indicating the stability of the AgNPs. All of the synthesized colloidal solutions were characterized in terms of Z-average, zeta potential, and polydispersity index (PDI) by dynamic light scattering (DLS) analysis (Table 1).

The hydrodynamic diameter of the AgNPs varied between 20.2 nm and 94.9 nm. With the exception of one experimental condition (0.05% at pH 11), there seemed to be a trend of increase in hydrodynamic size with increasing polysaccharide

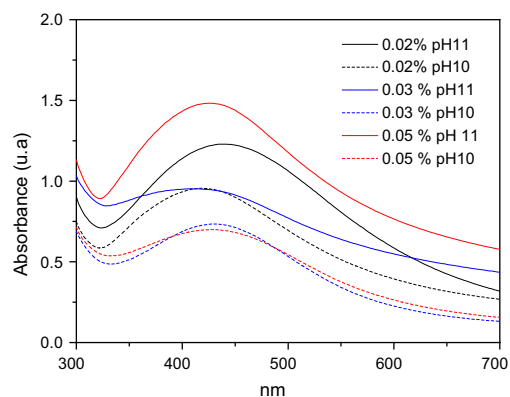


Figure 1 UV–vis spectrum for AgNPs synthesized in different conditions.

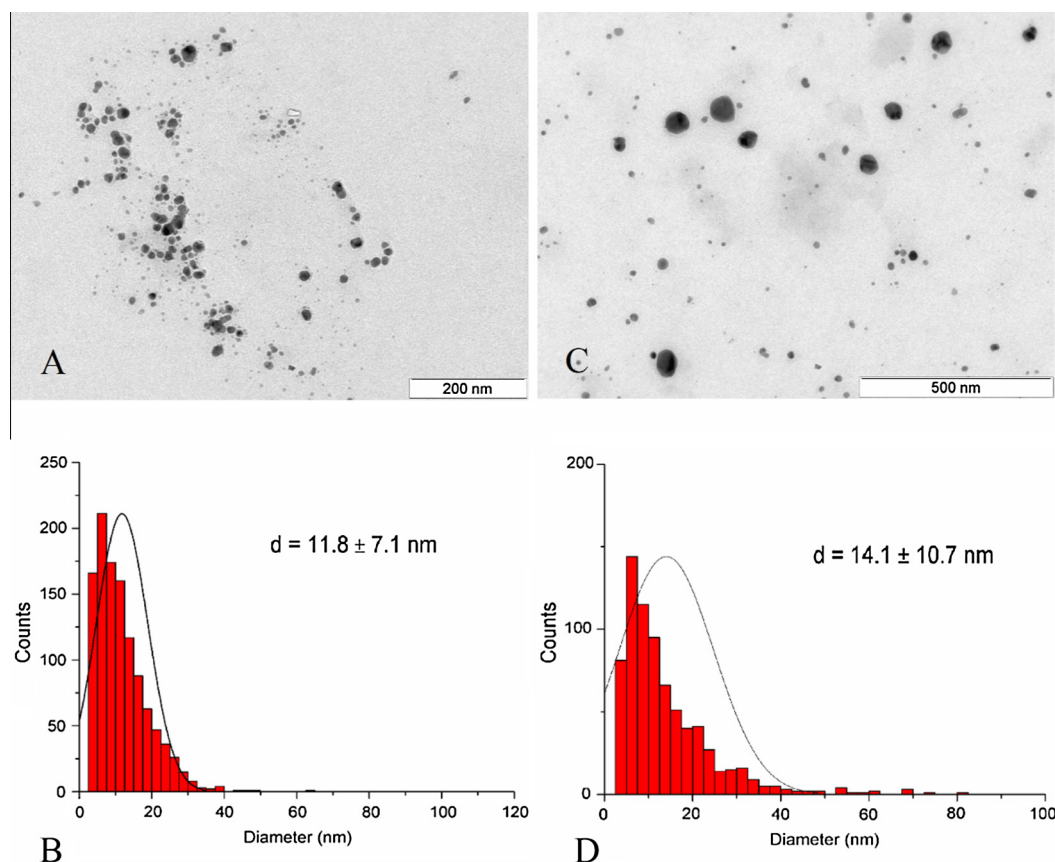


Figure 2 TEM images and histogram of the size distribution for silver nanoparticles: AgNPs obtained at pH 11 (A and B); AgNPs obtained at pH 10 (C and D).

Table 1 Polysaccharide concentration, size, PDI and zeta potential of AgNPs obtained at different pH.

	pH 10			pH 11		
Polysaccharide concentration (g/ml)	0.02%	0.03%	0.05%	0.02%	0.03%	0.05%
Hydrodynamic diameter (nm)	58.7	87.7	94.9	20.2	64.4	54.2
PDI	0.66	0.68	0.35	0.54	0.54	0.45
Zeta potential (mv)	-29.5 ± 0.6	-28.7 ± 0.7	-30.5 ± 0.3	-31.4 ± 0.5	-29.5 ± 0.7	-31.7 ± 0.4

*PDI: Polydispersity Index.

concentration. This finding might indeed reflect an increase in size of the synthesized NPs, or a change in the aggregation state of the particles or polysaccharide coating. Taking the UV-Vis spectra results into consideration, in which there was a blue shift with increasing polysaccharide concentration, a significant increase in particle size seems unlikely, as this would suggest a red shift in the plasmonic band instead of a blue shift.

Therefore, the most likely explanations for this increase in hydrodynamic size at higher polysaccharide concentrations include either a slight increase in the number of aggregates present (since DLS is a technique that is very sensitive to the presence of aggregates), or a more extensive polysaccharide coating around the particles. These options seem even more likely, considering the facts that the recorded TEM diameters were significantly lower than the corresponding hydrodynamic sizes

(Table 1 and Fig. 2), and that TEM measurements were limited to the inorganic silver core, whereas DLS measurements included the additional polysaccharide coating. This polysaccharide coating functioned as a type of polymeric capping agent, characterized by high molecular weight, and capable of significantly shifting the hydrodynamic radius to higher values relative to the size of the inorganic core.

An increase in pH affected a decrease in the hydrodynamic diameter of the AgNPs. This could have occurred because a smaller number of free H^+ ions in solution are expected to result in a greater magnitude of zeta potential and a subsequent reduction in the tendency to form AgNP aggregates (Zhang and Wu, 2010). Indeed, all samples yielded a negative zeta potential, suggesting that AgNPs were coated with the polysaccharide that is responsible for electrostatic stabilization of the colloidal solution. In addition, a slightly more negative

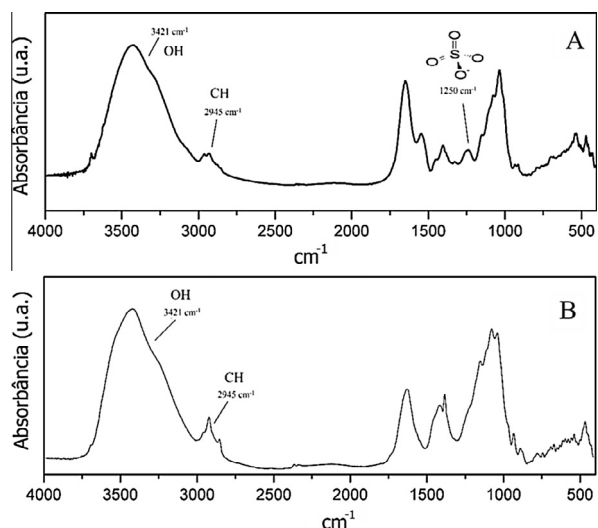


Figure 3 FTIR analysis of native polysaccharide (A) and AgNPs (B).

zeta potential was observed for samples with higher polysaccharide concentrations. Syntheses performed at high pHs were expected to result in more negative zeta potential values when the polysaccharide concentration was kept constant.

Regarding the PDI, values ranged between 0.35 and 0.68, with a clear trend of decreasing values with increasing polysaccharide concentration. This behavior is reflective of a reduction in the dispersion of the AgNPs at high polysaccharide concentrations. It also reflects typical behavior in NP synthesis, wherein increasing amounts of the capping agent

result in more monodisperse populations owing to simultaneous restriction of particle growth and impairment of the Ostwald ripening phenomena, which can broaden particle size distribution. It is clear that as the pH value increases, the sizes of the particles decrease and the nanoparticles have narrower size distribution. This difference can be attributed to the difference in the reduction rate of the precursor and poor balance between nucleation and growth processes.

The infrared spectroscopic analysis was used to characterize the extracted polysaccharide and the synthesized AgNPs. The infrared spectra of both polysaccharide and AgNPs are presented in Fig. 3, showing characteristic bands that can be attributed to the stretching vibration of OH and CH groups appearing at 3421 cm⁻¹ and 2945 cm⁻¹, respectively. The bands at 2945 and 2856 cm⁻¹ correspond to asymmetric and symmetric stretching vibrations of methylene groups, respectively. The stronger band found at 1626 cm⁻¹ could be assigned to characteristic asymmetrical stretch of carboxylate group. The symmetrical stretch of carboxylate group can be attributed to the bands present at 1429 and 1379 cm⁻¹. Among the functional groups of the polysaccharide, the presence of a small percentage of sulfate was confirmed by the existence of a band at 1250 cm⁻¹ (Wijesekara et al., 2011). However, this band was not evident with that of AgNPs (Fig. 3B). This finding can be due to the involvement of the sulfate group in binding to the NP surface, which could change the available vibrational frequencies of the group and shift the band to other regions. In the IR spectrum of nanoparticles small shifts in the polyols and alcoholic groups (1153–1163 cm⁻¹ and 1040–1028 cm⁻¹) were observed suggesting that the reduction of the silver ions is coupled to the oxidation of the hydroxyl and carbonyl groups.

Table 2 Minimum inhibitory concentrations (MICs) of AgNPs (μM), AgNO₃ (μM) and *G. Birdiae* (GB) (μg/mL) for *S. aureus* and *E. coli*.

Bacterial strains	AgNPs						Controls	
	pH10 0.02%	pH11 0.02%	pH10 0.03%	pH11 0.03%	pH10 0.05%	pH11 0.05%	AgNO ₃	GB
<i>S. aureus</i>	157.5	137.5	> 150	150	162.5	81.2	125	> 125
<i>E. coli</i>	78.7	34.3	75	37.5	81.2	40.6	62.5	> 125

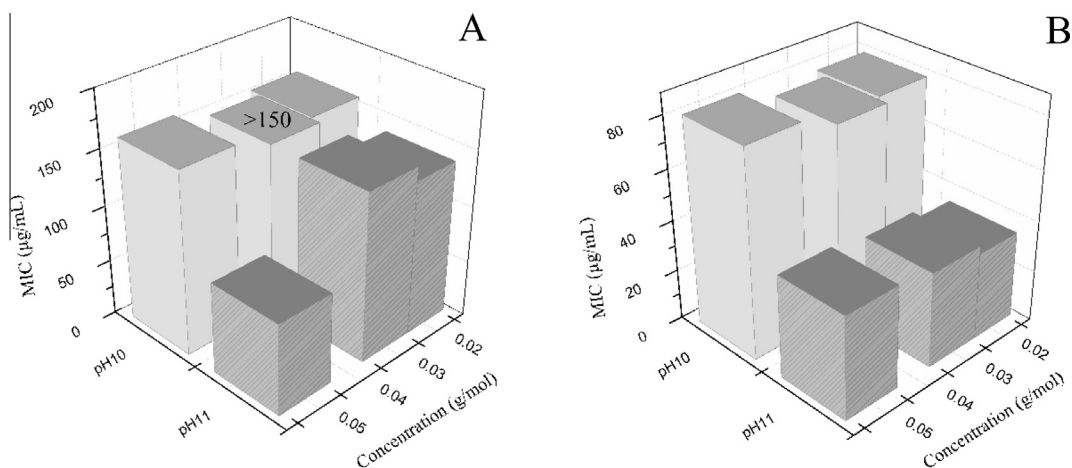


Figure 4 Minimum inhibitory concentration (MIC) for Silver nanoparticles obtained at different polysaccharide concentrations and pH: (A) *S. aureus* and (B) *E. coli*.

The small hydrodynamic diameters of AgNPs facilitate the potential for action against bacteria. Hamouda and Baker (2000) suggested that the small sizes of nanoparticles facilitated their bactericidal activity, by enabling them to easily permeate bacterial membranes. Furthermore, Baker et al. (2005) reported that small particles with relatively large contact areas (such as spherical nanoparticles) showed greater efficacy against bacteria, in comparison with large particles. With this in mind and considering the fact that AgNPs are typically reported to have considerable anti-bacterial activity, we evaluated their effects on bacterial growth. Two representative bacterial strains were selected to test the antimicrobial activity of the AgNPs: *S. aureus* (Gram-positive) and *E. coli* (Gram-negative). The results showed that the antibacterial effects of AgNPs against *E. coli* were higher than those against *S. aureus*. This finding could be attributed to differences in the composition of the cell wall between Gram-positive and Gram-negative bacteria (Guzman et al., 2012).

All samples showed antimicrobial activity against *E. coli* (Table 2). Antimicrobial action of various AgNPs samples against *S. aureus* was not significantly different because this type of bacteria has a thicker peptidoglycan layer making it difficult to absorb the AgNPs into their cytoplasm, a fact that is supported by previous studies (Pal et al., 2007). Greater antibacterial effects were observed among AgNPs synthesized with a polysaccharide concentration of 0.05% (pH 11). These samples presented the highest absorbance levels among all the synthesized AgNPs, which can be related to more optimal formation of nanoparticles (Fig. 4).

4. Conclusion

In the present study, we demonstrated the stable green synthesis of an AgNP solution with red algae reducing and stabilizing agent. The resulted particles exhibited favorable characteristics, including the spherical shape, hydrodynamic diameter between 20.3 nm and 94.9 nm and negative zeta potential. The synthesized AgNPs showed antibacterial activity with greater efficacy against Gram-negative bacteria, probably due to the shape and the size of AgNP. This kind of study may also serve as a model for the future preparation of nano-medicines or for targeted algal drug delivery.

Acknowledgments

The authors gratefully acknowledge financial support from CAPES and FAPESP; and Prof. Janaina de Araújo Sousa Santiago-UFPI (Federal University of Piauí) for the algae identified.

The authors gratefully thanks to FCT for the post-doctoral fellowship SFRH/BPD/84018/2012.

The authors also acknowledge the CNPq and Capes for scholarship and financial aid.

References

- Abdel-Mohsen, A.M., Abdel-Rahman, R.M., Fouda, M.M.G., Vojtova, L., Uhrova, L., Hassan, A.F., Al-Deyab, S.S., El-Shamy, I.E., Jancar, J., 2014. Preparation, characterization and cytotoxicity of schizophyllan/silver nanoparticle composite. *Carbohydr. Polym.* 102, 238–245. <http://dx.doi.org/10.1016/j.carbpol.2013.11.040>.
- Baker, C., Pradhan, A., Pakstis, L., Pochan, D.J., Shah, S.I., 2005. Synthesis and antibacterial properties of silver nanoparticles. *J. Nanosci. Nanotechnol.* 5, 244–249. <http://dx.doi.org/10.1166/jnn.2005.034>.
- Cardoso, V.S., Quelemes, P.V., Amorin, A., Primo, F., Gobo, G., Tedesco, A.C., Mafud, A.C., Mascarenhas, Y.P., Corrêa, J., Kuckelhaus, S., Eiras, C., Leite, J., Silva, D., dos Santos Júnior, J., 2014. Collagen-based silver nanoparticles for biological applications: synthesis and characterization. *J. Nanobiotechnol.* 12, 1–9. <http://dx.doi.org/10.1186/s12951-014-0036-6>.
- Carneiro, J.G., Rodrigues, J.A.G., Teles, F.B., Cavalcante, A.B.D., Benevides, N.M.B., 2014. Analysis of some chemical nutrients in four Brazilian tropical seaweeds. *Acta Sci. Biol.* 36, 137–145. <http://dx.doi.org/10.4025/actasciobiolsci.v36i2.19328>.
- Chattopadhyay, K., Ghosh, T., Pujol, C.A., Carlucci, M.J., Damonte, E.B., Ray, B., 2008. Polysaccharides from *Gracilaria corticata*: sulfation, chemical characterization and anti-HSV activities. *Int. J. Biol. Macromol.* 43, 346–351. <http://dx.doi.org/10.1016/j.ijbiomac.2008.07.009>.
- Chen, J., Wang, J., Zhang, X., Jin, Y., 2008. Microwave-assisted green synthesis of silver nanoparticles by carboxymethyl cellulose sodium and silver nitrate. *Mater. Chem. Phys.* 108, 421–424. <http://dx.doi.org/10.1016/j.matchemphys.2007.10.019>.
- Coura, C.O., de Araújo, I.W.F., Vanderlei, E.S.O., Rodrigues, J.A.G., Quinderé, A.L.G., Fontes, B.P., de Queiroz, I.N.L., de Menezes, D. B., Bezerra, M.M., e Silva, A.A.R., Chaves, H.V., Jorge, R.J.B., Evangelista, J.S.A.M., Benevides, N.M.B., 2012. Antinociceptive and anti-inflammatory activities of sulphated polysaccharides from the red seaweed *Gracilaria cornea*. *Basic Clin. Pharmacol. Toxicol.* 110, 335–341. <http://dx.doi.org/10.1111/j.1742-7843.2011.00811.x>.
- Diallo, A., Beye, A.C., Doyle, T.B., Park, E., Maaza, M., 2015. Green synthesis of Co₃O₄ nanoparticles via *Aspalathus linearis*: physical properties. *Green Chem. Lett. Rev.* 8, 30–36. <http://dx.doi.org/10.1080/17518253.2015.1082646>.
- El-Rafie, H.M., El-Rafie, M.H., Zahran, M.K., 2013. Green synthesis of silver nanoparticles using polysaccharides extracted from marine macro algae. *Carbohydr. Polym.* 96, 403–410. <http://dx.doi.org/10.1016/j.carbpol.2013.03.071>.
- Gils, P.S., Ray, D., Sahoo, P.K., 2010. Designing of silver nanoparticles in gum arabic based semi-IPN hydrogel. *Int. J. Biol. Macromol.* 46, 237–244. <http://dx.doi.org/10.1016/j.ijbiomac.2009.12.014>.
- Guzman, M., Dille, J., Godet, S., 2012. Synthesis and antibacterial activity of silver nanoparticles against Gram-positive and Gram-negative bacteria. *Nanomed. Nanotechnol. Biol. Med.* 8, 37–45. <http://dx.doi.org/10.1016/j.nano.2011.05.007>.
- Hamouda, T., Baker Jr., J.R., 2000. Antimicrobial mechanism of action of surfactant lipid preparations in enteric Gram-negative bacilli. *J. Appl. Microbiol.* 89, 397–403. <http://dx.doi.org/10.1046/j.1365-2672.2000.01127.x>.
- Kim, S.T., Lee, Y.-J., Hwang, Y.-S., Lee, S., 2015. Study on aggregation behavior of Cytochrome C-conjugated silver nanoparticles using asymmetrical flow field-flow fractionation. *Talanta* 132, 939–944. <http://dx.doi.org/10.1016/j.talanta.2014.05.060>.
- Konwarh, R., Karak, N., Sawian, C.E., Baruah, S., Mandal, M., 2011. Effect of sonication and aging on the templating attribute of starch for “green” silver nanoparticles and their interactions at bio-interface. *Carbohydr. Polym.* 83, 1245–1252. <http://dx.doi.org/10.1016/j.carbpol.2010.09.031>.
- Kora, A.J., Sashidhar, R.B., Arunachalam, J., 2010. Gum kondagogu (*Cochlospermum gossypium*): a template for the green synthesis and stabilization of silver nanoparticles with antibacterial application. *Carbohydr. Polym.* 82, 670–679. <http://dx.doi.org/10.1016/j.carbpol.2010.05.034>.
- Maciel, J., Chaves, L., Souza, B., Teixeira, D., Freitas, A., Feitosa, J., Depaula, R., 2008. Structural characterization of cold extracted fraction of soluble sulfated polysaccharide from red seaweed *Gracilaria birdiae*. *Carbohydr. Polym.* 71, 559–565. <http://dx.doi.org/10.1016/j.carbpol.2007.06.026>.

- Mohanty, S., Mishra, S., Jena, P., Jacob, B., Sarkar, B., Sonawane, A., 2012. An investigation on the antibacterial, cytotoxic, and antibiofilm efficacy of starch-stabilized silver nanoparticles. *Nanomed. Nanotechnol. Biol. Med.* 8, 916–924. <http://dx.doi.org/10.1016/j.nano.2011.11.007>.
- MubarakAli, D., Thajuddin, N., Jeganathan, K., Gunasekaran, M., 2011. Plant extract mediated synthesis of silver and gold nanoparticles and its antibacterial activity against clinically isolated pathogens. *Colloids Surf. B Biointerfaces* 85, 360–365. <http://dx.doi.org/10.1016/j.colsurfb.2011.03.009>.
- Nair, L.S., Laurencin, C.T., 2007. Silver nanoparticles: synthesis and therapeutic applications. *J. Biomed. Nanotechnol.* 3, 301–316.
- Padalia, H., Moteriya, P., Chanda, S., 2015. Green synthesis of silver nanoparticles from marigold flower and its synergistic antimicrobial potential. *Arab. J. Chem.* 8, 732–741. <http://dx.doi.org/10.1016/j.arabjc.2014.11.015>.
- Pal, S., Tak, Y.K., Song, J.M., 2007. Does the antibacterial activity of silver nanoparticles depend on the shape of the nanoparticle? A study of the Gram-negative bacterium *Escherichia coli*. *Appl. Environ. Microbiol.* 73, 1712–1720. <http://dx.doi.org/10.1128/AEM.02218-06>.
- Quelemes, P., Araruna, F., de Faria, B., Kuckelhaus, S., da Silva, D., Mendonça, R., Eiras, C., Soares, M. dos S., Leite, J.R., 2013. Development and antibacterial activity of cashew gum-based silver nanoparticles. *Int. J. Mol. Sci.* 14, 4969–4981. <http://dx.doi.org/10.3390/ijms14034969>.
- Souza, B.W.S., Cerqueira, M.A., Bourbon, A.I., Pinheiro, A.C., Martins, J.T., Teixeira, J.A., Coimbra, M.A., Vicente, A.A., 2012. Chemical characterization and antioxidant activity of sulfated polysaccharide from the red seaweed *Gracilaria birdiae*. *Food Hydrocoll.* 27, 287–292. <http://dx.doi.org/10.1016/j.foodhyd.2011.10.005>.
- Sone, B.T., Manikandan, E., Gurib-Fakim, A., Maaza, M., 2015. Sm_2O_3 nanoparticles green synthesis via *Callistemon viminalis* extract. *J. Alloys Compd.* 650, 357–362. <http://dx.doi.org/10.1016/j.jallcom.2015.07.272>.
- Thakkar, K.N., Mhatre, S.S., Parikh, R.Y., 2010. Biological synthesis of metallic nanoparticles. *Nanomed. Nanotechnol. Biol. Med.* 6, 257–262. <http://dx.doi.org/10.1016/j.nano.2009.07.002>.
- Thema, F.T., Beukes, P., Gurib-Fakim, A., Maaza, M., 2015a. Green synthesis of Montepelite CdO nanoparticles by *Agathosma betulina* natural extract. *J. Alloys Compd.* 646, 1043–1048. <http://dx.doi.org/10.1016/j.jallcom.2015.05.279>.
- Thema, F.T., Manikandan, E., Dhlamini, M.S., Maaza, M., 2015b. Green synthesis of ZnO nanoparticles via *Agathosma betulina* natural extract. *Mater. Lett.* 161, 124–127. <http://dx.doi.org/10.1016/j.matlet.2015.08.052>.
- Thovhogi, N., Diallo, A., Gurib-Fakim, A., Maaza, M., 2015. Nanoparticles green synthesis by *Hibiscus Sabdariffa* flower extract: main physical properties. *J. Alloys Compd.* 647, 392–396. <http://dx.doi.org/10.1016/j.jallcom.2015.06.076>.
- Tran, H.V., Tran, L.D., Ba, C.T., Vu, H.D., Nguyen, T.N., Pham, D. G., Nguyen, P.X., 2010. Synthesis, characterization, antibacterial and antiproliferative activities of monodisperse chitosan-based silver nanoparticles. *Colloids Surf. A Physicochem. Eng. Asp.* 360, 32–40. <http://dx.doi.org/10.1016/j.colsurfa.2010.02.007>.
- Venkatpurwar, V., Pokharkar, V., 2011. Green synthesis of silver nanoparticles using marine polysaccharide: study of in-vitro antibacterial activity. *Mater. Lett.* 65, 999–1002. <http://dx.doi.org/10.1016/j.matlet.2010.12.057>.
- Vigneshwaran, N., Nachane, R.P., Balasubramanya, R.H., Varadarajan, P.V., 2006. A novel one-pot “green” synthesis of stable silver nanoparticles using soluble starch. *Carbohydr. Res.* 341, 2012–2018. <http://dx.doi.org/10.1016/j.carres.2006.04.042>.
- Wijesekara, I., Pangestuti, R., Kim, S.-K., 2011. Biological activities and potential health benefits of sulfated polysaccharides derived from marine algae. *Carbohydr. Polym.* 84, 14–21. <http://dx.doi.org/10.1016/j.carbpol.2010.10.062>.
- Xia, N., Cai, Y., Jiang, T., Yao, J., 2011. Green synthesis of silver nanoparticles by chemical reduction with hyaluronan. *Carbohydr. Polym.* 86, 956–961. <http://dx.doi.org/10.1016/j.carbpol.2011.05.053>.
- Zhang, Z., Wu, Y., 2010. Investigation of the NaBH_4 -induced aggregation of Au nanoparticles. *Langmuir* 26, 9214–9223. <http://dx.doi.org/10.1021/la904410f>.
- Zhao, J., Pinchuk, A.O., McMahon, J.M., Li, S., Ausman, L.K., Atkinson, A.L., Schatz, G.C., 2008. Methods for describing the electromagnetic properties of silver and gold nanoparticles. *Chem. Soc. Rev.* 41, 1710–1720.